Received: 24 July 2018 | Revised: 28 March 2020 | Accepted: 30 April 2020

DOI: 10.1111/jfr3.12623

ORIGINAL ARTICLE

CIWEM Chartered Institution of Water and Environmental Management | Journal of Flood Risk Management | WILEY

Methodology for future flood assessment in terms of economic damage: Development and application for a case study in Nepal

Marie Delalay[1] | **Alan D. Ziegler**[1] | **Mandira Singh Shrestha**[2] | **Vik Gopal**[3]

[1]Geography Department, National University of Singapore, Singapore, Singapore

[2]International Center for Integrated Mountain Development (ICIMOD), Kathmandu, Nepal

[3]Department of Probability and Statistics, National University of Singapore, Singapore, Singapore

Correspondence
Marie Delalay, Geography Department, National University of Singapore, 5 Arts Link, Block AS3, Singapore 117570, Singapore.
Email: mariesdelalay@gmail.com

Abstract

To address the lack of adequate measures for flood risk reduction in Nepal, where recurrent flood-related hazards have had grave consequences for many people over the past decades, we develop a flood risk assessment model for a study area in the Sindhupalchok District. The model considers direct and indirect damages that are assigned to four asset categories (hydropower plants, roads, houses, and farmlands) and two scenarios (low-exposure-low-flood and high-exposure-high-flood scenarios). Model results indicate the following: (a) the planned expansion of hydropower plants reflected in the high exposure scenario is responsible for a substantial increase of economic damage compared with the low scenario and (b) for both scenarios, flood damage is largely related to road closures, which result in the loss of income for villagers and the loss of customs revenues. As this study aims both to provide methods for the assessment of flood risk and to demonstrate them in a case study, we discuss future work related to model-based flood risk assessments that are needed towards flood risk reduction in Nepal.

KEYWORDS

flood damages, modeling, risk assessment

1 | INTRODUCTION

Flood risk in Nepal, a country known for recurrent and devastating floods, landslides, and earthquakes, has recently increased because of changes of the spatial/temporal distribution of cumulative precipitation, economic/demographic growth, and a lack of adequate measures for flood risk reduction (CBS, 2014c; CRED, 2016; Gautam, Prajapati, Paterno, Bhetwal, & Neupane, 2016; Jaquet et al., 2015; Malego & Upreti, 2015). Flood-related hazards in Nepal include rainfall-induced floods, glacial lake outburst floods (GLOFs) and landslide lake outburst floods (LLOFs), and flood-induced landslides (Bookhagen & Burbank, 2006; Dahal & Bhandary, 2013; Dhakal, 2015; Feyen, Dankers, & Bódis, 2011; Gaire, Castro Delgado, & Arcos González, 2015; Kansakar, Hannah, Gerrard, & Rees, 2004; Muis, Gueneralp, Jongman, Aerts, & Ward, 2015; Schwanghart, Worni, Huggel, Stoffel, & Korup, 2016). The latter are caused by landslides at the river side that are triggered by the scouring of river banks during high-water flows (Chen et al., 2013; Devkota et al., 2013; Kayastha, Dhital, & DE Smedt, 2013).

Recurrent floods and hazards cascading from floods have had grave consequences for many people in Nepal over the past decades (CBS, 2014c; CRED, 2016; Gautam et al., 2016; Jaquet et al., 2015; Malego & Upreti, 2015). The mean annual economic cost of damage to infrastructure and livelihoods associated with floods and landslides in Nepal for the period 1983–2010 amounts to 232 million USD, with 1987 and 1993 being the costliest years (1.6 and 1.2 billion USD, respectively) (IDS-Nepal et al., 2014). In 2015 and 2016, a total of 244 flood events reported in Nepal were estimated to have damaged 2,600 buildings, incurred economic damage of 47 million Nepali rupees (NPR; 0.47 million USD with the exchange rate of Bloomberg Markets, 2017), and affected 7,100 families (Neupane et al., 2018).

The risk of the occurrence of a flood disaster, or simply flood risk, emerges from the combination of the occurrence of flood-related hazards and the vulnerability to these hazards (Kelman, 2015). In this work, flood risk is represented by direct and indirect damages caused by floods and flood-induced landslides. The extent of damage from future floods is commonly estimated in mathematical models in which flood risk is quantified in terms of economic damage. In this paper, these types of mathematical models are referred to as flood risk assessment models (FRAMs). While FRAMs are widely produced and used by academics, governmental agencies, and the insurance industry (Gerl, Kreibich, Franco, Marechal, & Schröter, 2016; Grossi, Kunreuther, & Patel, 2005; United Nations, 2015), we have not found one developed for Nepal, although various assessments of flood risk have been made in terms of flood depth and vulnerability for the country or various parts of it (e.g., ADPC, 2015; Khanal, Hu, & Mool, 2015; Rimal, Baral, Stork, Paudyal, & Rijal, 2015; Rounce, Mckinney, Lala, Byers, & Watson, 2016).

The lack of estimates of the economic value associated with future flood damages hampers the ability of decision-makers to comprehend the urgency of the implementation of improved measures for flood risk reduction for the general population, businesses, and the Government of Nepal (Dixit, 2009). To address this inadequacy of measures for flood risk reduction, we develop a FRAM that expresses the risk of floods and flood-induced landslides in terms of economic damage for both a low and high exposure scenario. The model is applied for an area in the Sindhupalchok District of Nepal where recent and historical evidence suggests that both floods and flood-induced landslides are recurrent and destructive (Cook, Andermann, Gimbert, Hovius, & Adhikari, 2017; Regmi, Cui, Dhital, & Zou, 2016; Shrestha & Nakagawa, 2016).

2 | STUDY AREA

The 1,376 km^2 study area in the Sindhupalchok District is a part of the Koshi Basin, which includes regions of China, Nepal, and India. The study area, which is the Nepali part of the basin with the outlet of the Sunkoshi at Dolalghat, includes the Bhotekoshi Sub-Basin from Liping to Bahrabise (359 km^2) and the Balephi Sub-Basin down to Balephi Village (676 km^2) (map on the left in Figure 1).

The study area contains seven river reaches (i.e., longitudinal stretches of rivers defined for modeling purpose) that are considered in the FRAM (map on the right in Figure 1). In the Bhotekoshi Sub-Basin, two river reaches correspond to the precipitation- and glacier-fed Bhotekoshi; and another river reach corresponds to the precipitation-fed Chaku River. The fourth river reach is in the Balephi Sub-Basin and corresponds to the precipitation-fed Balephi River. The fifth river reach is the precipitation-fed Upper Sunkoshi. Finally, the Sunkoshi, which originates in Bahrabise (where the Upper Sunkoshi and the Bhotekoshi meet) and extends down to its confluence with the Indrawati River at Dolalghat, is split into two reaches at Balephi Village.

According to the Central Bureau of Statistics of the Government of Nepal (CBS, 2014a), the study area contains 37 of the 80 village development committees of the Sindhupalchok District, representing 127,520 of the 287,794 people in the district. The United Nations Development Program (UNDP, 2014) estimates an annual 2014 Gross National Income (GNI) per capita of 687 USD for the Sindhupalchok District, to which the income from agricultural activities contributes 50%. As per 2017, there are at least four major sources of income for the local population in the study area: agriculture, remittances, employment in retail trades, and jobs related to infrastructure construction and maintenance (Delalay et al., 2018). Until the closure of the customs station in Liping in 2015, income generated from road traffic (mainly the Araniko Highway) added significantly to the income for the local population, with many working as traders and porters, or in storage facilities, hotels, restaurants, and kiosks. The customs station was closed after damage during both the 2015 Gorkha Earthquake and the 2016 Bhotekoshi GLOF.

As of January 2017, there were seven existing HPPs of installed capacity >1 MW that were registered with the Department of Electricity Development of the Government of Nepal (DoED, 2017). In addition, the river corridors of the study area contained 11 plots of land where the DoED (2017) reported that HPPs could be developed in the future (map on the left in Figure 1). With an estimated 5 billion USD per annum at 2010 prices, the net economic value of potential HPPs in Nepal is substantial (Rasul, 2015).

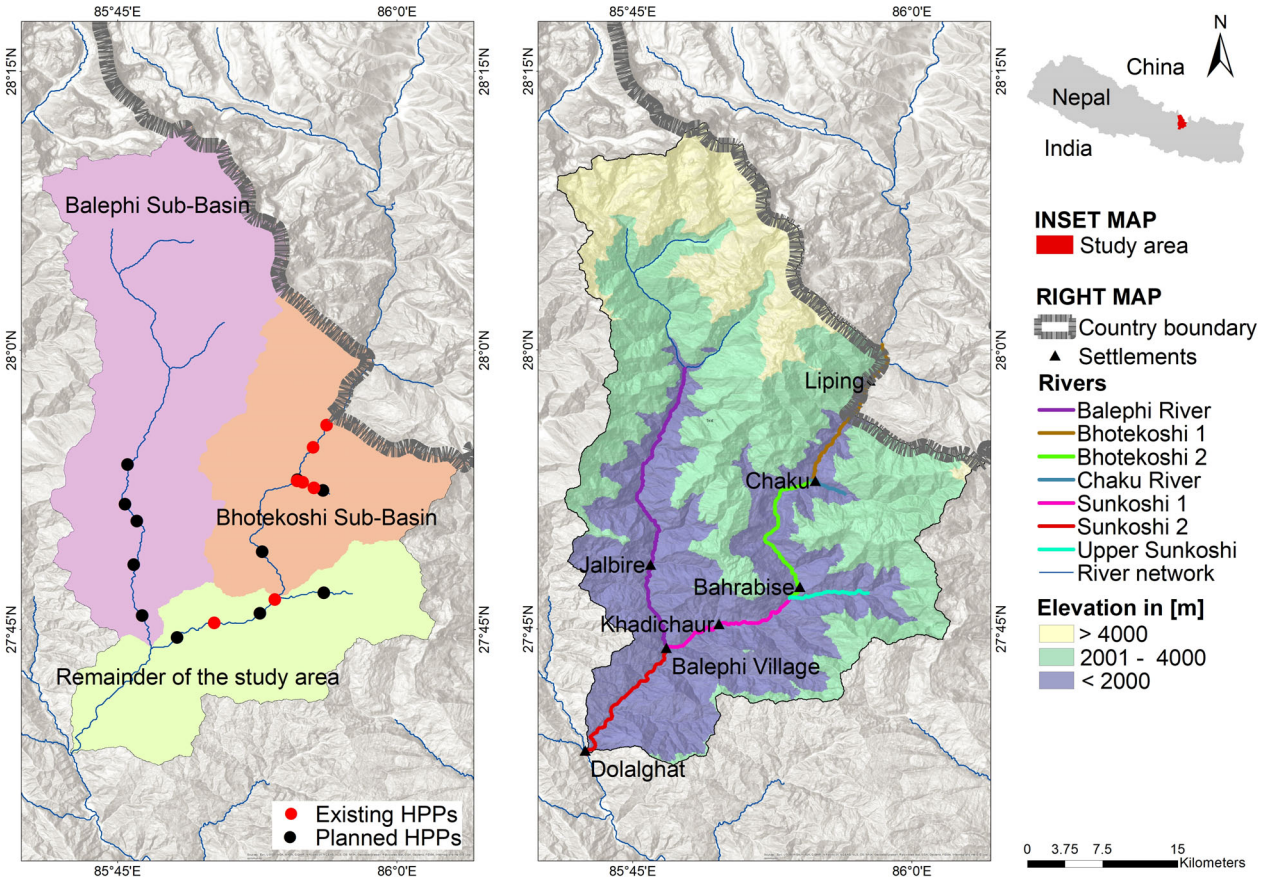

FIGURE 1 Study area. The left map shows the division of the study area into sub-basins, as well as the 7 existing (red dots) and 11 planned (black dots) hydropower plants (HPPs) as per the DoED (2017). The right map shows elevation ranges and settlements, as well as the seven river reaches

3 | METHODS

3.1 | Overview of existing methods

In the academic and grey literature, the implementation of FRAMs that quantify risk in terms of economic damage generally relies on the existence of a relationship between the magnitude of the hazard, exposure (which represents the portion of assets that flood-related hazards might incur direct damage to), and both the direct and indirect damages caused by the hazard (OECD, 2016; de Moel, VAN Alphen, & Aerts, 2009; Koks, Bočkarjova, Moel, & Aerts, 2014; Shaw & Rahman, 2015; Smith, 1994; Swiss Re, 2012). The methods used in FRAMs are highly heterogeneous and vary according to the purpose, constraints, and requirements of the model (Agoshkov, 2002). Despite this heterogeneity, FRAMs have generally three components in common: a hazard module, an asset module, and an aggregation module (Arnell, 1989; de Moel et al., 2009; de Moel et al., 2015; Grossi et al., 2005; Ligtvoet et al., 2013; Smith, 1981; Swiss Re, 2012; Woo, 2011). Many studies, for example those of McGrath, Bourgon, Proulx-Bourque, Nastev, and Abo El Ezz (2018), Muis et al. (2015), and Wilson et al. (2007), focus on the hazard module only.

In the hazard module, hazard raster layers either correspond with scenarios (each of which is possibly assigned a probability of occurrence) or are fully probabilistic (e.g., a probability distribution of water depth is computed for each pixel). In the asset module, in general, LULC raster layers are produced, and functions for each asset category that relate hazard magnitude and damage are derived. Damage functions that define the ratio between the damage by floods and the total economic value according to the water depth are an example of such functions (de Moel et al., 2009; Gerl et al., 2016; Smith, 1994).

Finally, the outputs of the hazard module and the asset module are combined in the aggregation module. This last module routinely includes Monte-Carlo simulations to convolute or marginalise probability distributions, for example, the distributions of water depth per pixel or the conditional distribution of damage ratio given the water depth. The calculation of indirect damage generally depends on the estimated value of direct

damage (Smith, 1994). In the aggregation module, flood risk can be quantified as the expected annual damage, which is calculated by integrating the loss exceedance curve (i.e., a mathematical function where damage depends on exceedance probability) as in Drab and Riha (2010).

In this work, we split our model into these three modules. Our modeling methods, described in detail in the following sections, draw conceptually from the general methods described in this section, and have been defined to align with the purpose, constraints, and requirements of our model.

3.2 | Underlying hazards, asset categories, scenarios, and model implementation

Again, the hazards underlying flood risk in our FRAM are floods (i.e., rainfall-induced floods, GLOFs, and LLOFs) and flood-induced landslides. We model the economic value of eight types of consequences of flood-related hazards, which are classified according to the damage type (direct and indirect damage) and the asset category (HPP, road, settlement, and farmland).

The modeled damage to the asset category HPP corresponds with damaged headworks and powerhouses (direct damage), as well as the loss of revenue due to the interruption of power generation (indirect damage). The modeled damage to the asset category road corresponds with the physical damage to roads (direct damage), as well as the loss of customs revenue due to road closures (indirect damage). The modeled damage to the asset category settlement corresponds with damaged houses (direct damage), as well as the loss of revenue for the local population due to road closures (indirect damage). Finally, the modeled damage to the category farmland corresponds with the loss of crop (direct damage), as well as the loss of revenue from subsequent harvests due to long-term damage to agricultural fields (indirect damage).

The indirect damage for all four asset categories is calculated for a time horizon of 2 years. Economic values are not discounted to present values because of the shortness of the time horizon. Economic values of damage are estimated for a low-flood-low-exposure scenario (called hereafter "low scenario") and a high-flood-high-exposure scenario (called hereafter "high scenario"). The low scenario includes the following inputs and parameters: (a) the baseline-flood extent raster layer derived in Delalay et al. (2018), representing low-magnitude floods; (b) the presence of seven HPPs, that is, the HPPs that exist as per January 2017 (DoED, 2017); and (c) a house value of 1.5 million NPR (15,000 USD), which corresponds to the 2017 value of a house and is estimated from interviews described in Delalay et al. (2018). The following inputs and parameters are used for the high scenario: (a) the high-extreme-flood extent raster layer in Delalay et al. (2018), representing high-magnitude floods; (b) the presence of 18 HPPs, which is the number of existing and planned HPPs as reported by the DoED (2017); and (c) a house value of 3 million NPR (30,000 USD; this value accounts for both demographic and economic developments).

The rationale for the definition of these scenarios is that while both an increase of the volume of river runoff and economic/demographic growth (e.g., construction of HPPs and higher standard of living of the population) are predicted for Nepal there are high uncertainties in their estimation (CBS, 2014b; CBS, 2014c; DoED, 2017; Gautam et al., 2016; Jaquet et al., 2015; Lutz, Immerzeel, Shrestha, & Bierkens, 2014; Malego & Upreti, 2015; Rimal et al., 2015; UNDP, 2014). Further, the model relies on scenarios because the flood raster layers do not provide information on either water depth of flooded areas or probabilities of occurrence, which impedes the use of damage functions and loss exceedance curves. Important in our definitions is that the terms "low" and "high" refer to the flood extent and the exposure, not to the flood risk.

This work relies on primary data collated during field work (including the interviews described in Delalay et al. (2018)) and secondary data. Essential information from interviews includes the following: (a) economic value per pixel for the asset categories HPP, road, and settlement and (b) the duration of road closures and disruption of HPP operations which result from environmental hazards. The secondary data comes from the following sources: Delalay et al. (2018) for the flood hazard raster layers; Delalay, Tiwari, Ziegler, Gopal, and Passy (2019) for the land-use and land-cover (LULC) raster layer; the International Center for Integrated Mountain Development (ICIMOD, 2017c) for the landslide database; the United States Geological Survey (USGS, 2017) for the 1 arc-second SRTM; and the DoED (2017) for the database of HPPs. The R (R Foundation, 2017) codes, as well as links to input and output data, are available in a GitHub repository (Delalay, 2018). All raster layers used and derived in the FRAM have a spatial resolution of 1 arc-second (about 30 m at real scale).

3.2.1 | Hazard module

In the hazard module, we include two flood raster layers that correspond with the baseline-flood and high-extreme-flood scenarios in Delalay et al. (2018). In that study, flood raster layers are derived for three scenarios using a

conceptual model that draws from a bathtub inundation model (McGrath et al., 2018; Muis et al., 2015; Wilson et al., 2007). In addition, the hazard module covers three steps that are involved in the derivation of raster layers of flood-induced landslides: (a) identifying the locations of the toes of potential flood-induced landslides; (b) estimating the landslide area; and (c) defining sampling weights.

The locations of the toes of potential flood-induced landslides are derived based on two inputs: (a) the flood raster layers and (b) the hydrological and geological variables that are known to condition landslides in Nepal (Devkota et al., 2013; Kayastha et al., 2013; Regmi et al., 2016). In our model, conditioning variables include the slope of the terrain, the distance to a river bend, and the presence of flood-water. Each toe of a potential flood-induced landslide is contained in a pixel. For each of the low-flood and high-flood scenarios, the locations of toes of potential flood-induced landslides are assumed to be in pixels that have the following properties: (a) they are adjacent to the outer bend of the river; (b) they have a slope $\geq 30\%$; and (c) they are flooded according to the flood raster layer for the flood scenario that is considered. The rationale for the first assumption is that the flow velocity is generally the fastest at the outer bend of a river bed. The second assumption relies on an estimated slope threshold at which landslides in Nepal are recurrent (Kargel, Leonard, & Shugar, 2016). The third assumption enables the modeling of a causal link between floods and flood-induced landslides.

The location of a potential flood-induced landslide is constructed by defining both its orientation from its toe and its area. The orientation follows the tangent of the outer bend of the river. The area of all potential flood-induced landslides is assumed to be 14,000 m^2, which is an arithmetic mean derived from the landslide inventory of ICIMOD (2017b).

Sampling weights are contained in the raster layer of sampling weights of potential flood-induced landslides. The sampling weights are used in the aggregation module to identify a subset of potential flood-induced landslides and to simulate raster layers of actual flood-induced landslides. Sampling weights of potential flood-induced landslides depend on both the angle of river curvature and the lithology, as sampling weights are the normalised product of the so-called "rock weight" and "angle weight."

The sampling weight associated with a potential flood-induced landslide increases with a higher fragility of rocks in the geological formation at the toe of the landslide. As such, the rock weight depends on the predominant rock at the location of the toe of the flood-induced landslide. The rock weights take discrete values equal to 0.1, 0.2, 0.3, or 0.4 (the higher the value, the more fragile the rock). The map of geological formations is supplied by ICIMOD (2017a). Also, the sampling weight increases with a wider angle of the adjacent river bend. Angle weights have discrete values equal to 0.33 or 0.67 (the higher the value, the wider the angle).

3.3 | Asset module

In the asset module, value raster layers are defined in two steps. First, the LULC raster layer derived in Delalay et al. (2019), which already contains the land-use types "settlement" and "farmland," is refined to include the land-use types "HPP" and "road" for both the low-exposure and high-exposure scenarios. The refined LULC raster layer includes 7 HPPs for the low-exposure scenario and 18 HPPs for the high-exposure scenario. Shapefile layers of polylines of roads are digitised based on Google Earth images (Digital Globe, 2017), validated with GPS measurements taken in April 2017, and converted into raster layers.

For each of the refined LULC raster layers, an economic value is assigned to each pixel that corresponds with the land-use "HPP," "road," "settlement," and "farmland." The economic value per pixel p and asset category y is denoted $EV_{p,\,y}$ for $y = \{\text{road, farmland}\}$. If a distinction is made for the exposure scenario k, it is denoted $EV_{k,\,p,\,y}$, where $y = \{\text{HPP, settlement}\}$. These values are estimated from Bhandari, Bhattarai, and Aryal (2015), CBS (2014c), and CBS (2013) for farmland. For the other asset categories, these values are based on the analysis of interviews that are presented in Delalay et al. (2018).

For the calculation of $EV_{p,\,\text{HPP}}$, the total value of an HPP per MW is estimated at 164 million NPR (1.6 million USD) for both exposure scenarios. For the calculation of $EV_{p,\,\text{road}}$, the replacement cost per kilometre of roads is estimated to be 100 million NPR (1 million USD). For the calculation of $EV_{\text{low},\,p,\,\text{settlement}}$ and $EV_{\text{high},\,p,\,\text{settlement}}$, the economic value of a house is set equal to 1.5 million NPR (15,000 USD) and 3 million NPR (30,000 USD), respectively. For the calculation of $EV_{p,\,\text{farmland}}$, the value of crop per km^2 of farmland is set equal to 4.9 million NPR (49,000 USD), which is an estimation of the farm gate crop value of a mix of millet, rice, maize, and wheat.

Other outputs of this module are the value of the percentage of affected exposure (PAE), as well as the parameters of the theoretical distribution function that is assumed for the mean damage degree (MDD). The ratio between the value of the direct damage and the value of the exposure (which represents the portion of assets that flood-related hazards might incur direct damage to) is set equal to the product of the PAE and the MDD as proposed by Swiss Re (2003). This approach considers that only a part of the total exposure is affected by floods and flood-induced landslides; this ratio is the PAE. Subsequently, the

affected exposure is in general only partially damaged. This degree of damage to the affected exposure is the MDD.

In the model, the PAE is set at 7% for all asset categories; and two assumptions related to the MDDs are made: (a) the MDDs follow a Beta distribution (for the domain of this distribution is between 0 and 100%) with $\alpha = \beta = 4$ (such that the mean of the distribution is 50% and the distribution is symmetric) and (b) MDDs are independent within and across asset categories.

3.3.1 | Aggregation module

The outputs of the aggregation module are probability distributions that are generated by using Monte-Carlo simulations. For each combination of a flood scenario $i = 1, 2$ (i.e., low-flood and high-flood), an exposure scenario $k = \{\text{low, high}\}$, a simulation $j = 1, ..., 1000$, and an asset category $y = \{\text{HPP, road, settlement, farmland}\}$, both direct damage and indirect damage are simulated.

For each scenario, two pseudo-random draws (i.e., sampling from probability distributions that are not a uniform distribution) are used to simulate each of the 1,000 raster layers of actual flood-induced landslides. First, the actual count of flood-induced landslides (denoted X) is sampled from a Poisson distribution, the parameter λ of which is the product of the following terms: (a) the ratio between the mean count of landslides and the maximum count of landslides in the study area, as per the landslide inventory of ICIMOD (2017b) and (b) the count of all potential flood-induced landslides in the raster layer of potential flood-induced landslides (see above for the derivation of this raster layer) for the flood scenario considered.

The second pseudo-random draw is used to sample the locations of these X flood-induced landslides from a discrete density function of the potential flood-induced landslides. The discrete density function is derived from the raster layer of sampling weights of flood-induced landslides. For the low-flood scenario (respectively the high-flood scenario), the hazard raster layer for any of the 1,000 simulations is obtained from the union of the raster layer of actual flood-induced landslides for that simulation and the flood raster layer representing low-magnitude floods (respectively high-magnitude floods).

For each of the 1,000 simulations, the values of direct damage $DD_{i,\,j,\,y}$ or $DD_{i,\,j,\,k,\,y}$ if the direct damage varies according to the exposure scenario, are computed in five steps. First, for a simulation, an exposure raster layer is obtained from the intersection of the value raster layer and the hazard raster layer (Figure 2). Second, for each asset category, the number of pixels of exposure that are affected by the hazards, denoted N, is calculated as a portion (i.e., PAE = 7%) of the total number of exposure pixels. Third, the N pixels of affected exposure are randomly selected with equal probability. Fourth, MDDs are generated for all N selected pixels. Finally, for each of the N pixels, the economic value associated with the asset category of the pixel is multiplied by the MDD. These values are summed to obtain the economic values of direct damage for the simulation and asset category. The following equations describe the derivation of the direct damage:

$$\mathrm{DD}_{i,j,y} = \sum_{p=1}^{P} \mathbf{1}_{\mathrm{A}(y)} \cdot \mathrm{MDD}_{i,j,p} \cdot \mathrm{EV}_{p,y} \text{ for } y = \{\text{road, farmland}\} \tag{1}$$

$$\mathrm{DD}_{i,j,k,y} = \sum_{p=1}^{P} \mathbf{1}_{\mathrm{A}(y)} \cdot \mathrm{MDD}_{i,j,k,p} \cdot \mathrm{EV}_{k,p,y} \text{ for } y = \{\text{HPP, settlement}\} \tag{2}$$

where $p = 1, ..., P$ represent the pixels of the study area; $\mathbf{1}_{\mathrm{A}(y)}$ is the indicator function with A(y) the subset of all sampled pixels of exposure of the asset y (the sampled pixels depend on the PAE); $\mathrm{MDD}_{i,\,j,\,p}$ is the sampled MDD at pixel p for the flood scenario i and simulation j; $\mathrm{EV}_{p,\,y}$ is defined above; $\mathrm{MDD}_{i,\,j,\,k,\,p}$ is the sampled MDD at pixel p for the flood scenario i, exposure scenario k, and simulation j; and $\mathrm{EV}_{k,\,p,\,y}$ is defined above (Figure 3).

The calculation of indirect damage varies for each asset category. Indirect damage for the category HPP depends on the direct damage modeled for this asset category. In each of the 1,000 simulations, for each pixel where direct damage to HPPs with an MDD higher than 20% is modeled, indirect damage amounts to the value of 2 years of revenue from power generation. To obtain the two-year value, the mean 2-year revenue per MW of 47 million NPR (470,000 USD) is multiplied by the installed capacity of the HPP. No indirect damage to the HPP is modeled if the MDD related to the direct damage is equal to or lower than 20%. The economic value of indirect damage for HPPs is therefore calculated as follows:

$$\mathrm{ID}_{i,j,k,\mathrm{HPP}} = \sum_{p=1}^{P} \alpha \cdot \mathbf{1}_{\mathrm{A}} \cdot \mathrm{MW}_{p,k} \tag{3}$$

where α represents business interruption and is set equal to the mean two-year revenue per MW of 47 million NPR (470,000 USD); $\mathbf{1}_{\mathrm{A}}$ is the indicator function with A the subset of all sampled pixels of exposure of HPPs for which $\mathrm{MDD}_{i,\,j,\,\mathrm{HPP},\,p} > 20\%$ in Equation (2) and $\mathrm{MW}_{p,\,k}$ is the installed capacity of an HPP at pixel p for the exposure scenario k.

Indirect damage for the category road depends on the modeled direct damage for this category. In each of the

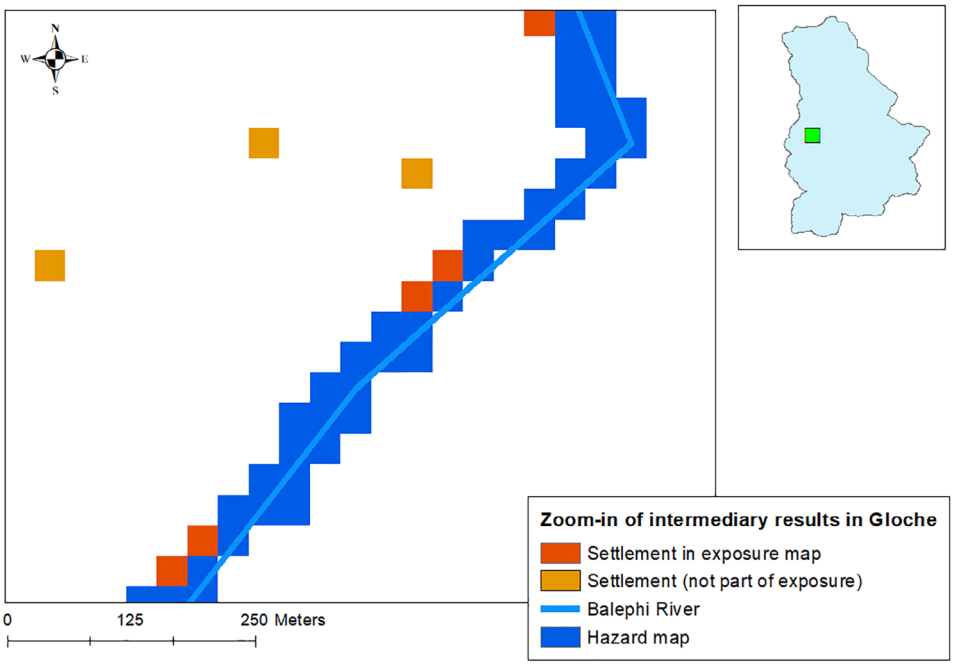

FIGURE 2 Derivation of the exposure raster layer for a simulation and a part of a settlement, Gloche (which is indicated in green in the inset map), assuming for illustration purpose the presence of one asset category only (settlement). Orange and red pixels indicate the land-use "settlement" as per the LULC raster layer. A settlement pixel is included in the exposure raster layer (red pixels) when it overlaps with a pixel of the hazard map that indicates the presence of a flood-related hazard

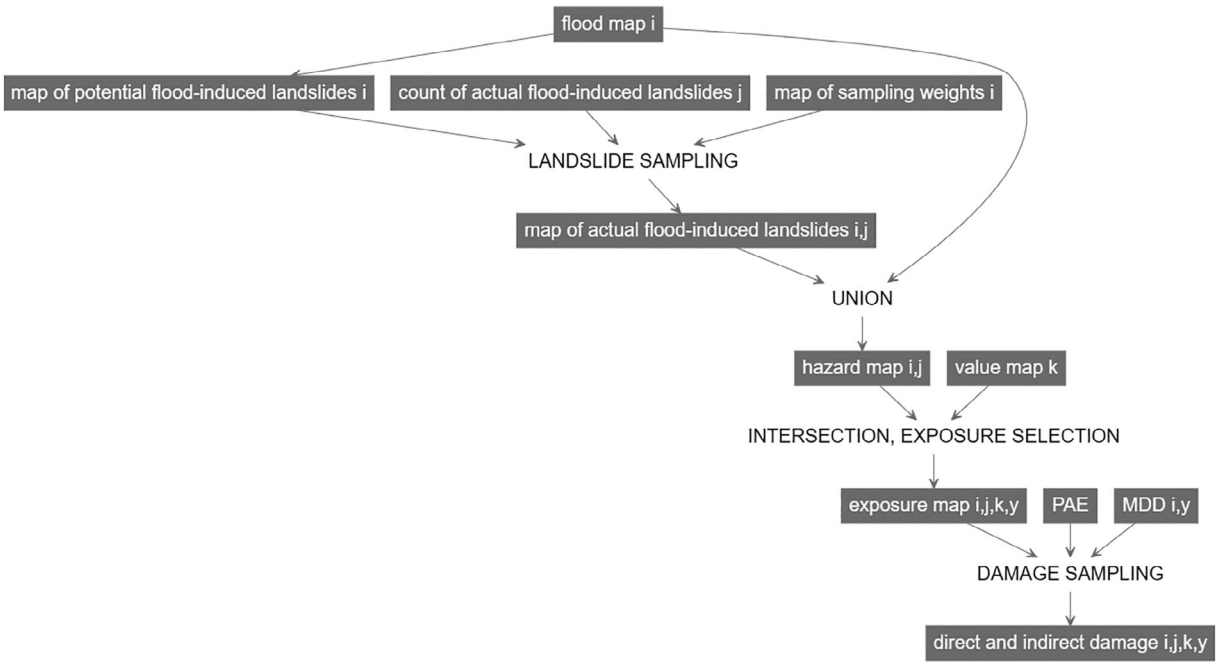

FIGURE 3 Modeling flowchart of the aggregation module. For each combination of flood scenario $i = 1, 2$ (i.e., low-flood and high-flood), exposure scenario $k = \{\text{low, high}\}$, simulation $j = 1, \ldots, 1{,}000$, and asset category $y = \{\text{HPP, road, settlement, farmland}\}$, both direct damage and indirect damage are simulated. The text in boxes represents input and output. The free text represents operations

1,000 simulations, the duration of road closures ranges between half a year and 2 years. This duration is calculated by assuming it to be linear with the direct damage to roads that is normalised with the 10%-quantile and 90%-quantile of direct damage to roads across all scenarios and all simulations. The duration of road closures is multiplied by an annual customs revenue of 3,600 million NPR (36 million USD) to compute the value of indirect damage. The economic value of indirect damage for the asset category road is therefore calculated as follows:

$$\begin{aligned} \mathrm{ID}_{i,j,\mathrm{road}} &= \beta \cdot \mathrm{RC}_{i,j} \\ &= \beta \cdot \left(0.5 + \frac{\mathrm{DD}_{i,j,\mathrm{road}} - \mathrm{DD}_{\cdot,\cdot,\mathrm{road};10\%}}{\mathrm{DD}_{\cdot,\cdot,\mathrm{road};90\%} - \mathrm{DD}_{\cdot,\cdot,\mathrm{road};10\%}} \cdot (2-0.5)\right) \end{aligned} \quad (4)$$

where β is the annual customs revenue of 3,600 million NPR (36 million USD); $RC_{i,\,j}$ represents the duration of road closures (between half a year and 2 years) for a flood scenario i and simulation j; $DD_{i,\,j,\,road}$ is defined in Equation (1); and $DD_{\cdot,\,\cdot,\,road;\,10\%}$ and $DD_{\cdot,\,\cdot,\,road;\,90\%}$ are the 10%-quantile and 90%-quantile of direct damage to roads across all scenarios and all simulations.

Indirect damage for the category settlement in each of the 1,000 simulations depends on the duration of road closures for the category road for the same simulation, as well as on the following assumptions derived from both census data in CBS (2014a) and data from interviews: (a) there are 22,600 households near roads and customs stations; (b) the business related to roads and customs is the main source of income for 20% of these households; and (c) each household earns from these activities 2000 NPR (20 USD) per day. Based on these numbers, the annual income of villagers from the business related to roads and customs is estimated at 3306 million NPR (33 million USD). This value is multiplied by the duration of road closures to obtain the value of indirect damage. The economic value of indirect damage for the asset category settlement is therefore calculated as follows:

$$ID_{i,j,\text{settlement}} = \gamma \cdot RC_{i,j} \tag{5}$$

where $RC_{i,\,j}$ is defined in Equation (4) and γ is the annual income of villagers from business related to roads and customs, which is estimated at 3306 million NPR (33 million USD).

Finally, for each combination of flood scenario and simulation, the economic value of indirect damage for the category farmland is set equal to the value of direct damage for this asset category multiplied by the time horizon of 2 years (i.e., two future annual harvests are assumed to be lost, in addition to the loss of harvest modeled as the direct damage to farmland). The economic value of indirect damage for the asset category farmland is therefore calculated as follows:

$$ID_{i,j,\text{farmland}} = \delta \cdot DD_{i,j,\text{farmland}} \tag{6}$$

where $DD_{i,\,j,\,\text{farmland}}$ is defined in Equation (1); and $\delta = 2$ is the number of future harvests that are assumed to be damaged.

4 | RESULTS

A first important model result is that the expansion of HPPs that is assumed in the high scenario is responsible for a substantial increase of modeled economic damage between the low scenario and the high scenario. Estimated total economic damage increases between the low scenario and the high scenario by a factor of 2.4 (Table 7), that is, from a mean of 58.8 million USD (Table 1) to 141.8 million USD (Table 4). Total damage to HPPs increases between the low scenario and the high scenario by a factor of 14.5 (the highest increase among the four asset categories; Table 7), from a mean of 1.5 million USD (Table 1) to 22 million USD (Table 4). For each scenario, a bar chart split by asset category and stacked by damage type is provided in Figure 4.

Because both the extent of hazards and the exposure value increase from the low scenario to the high scenario, it is useful to explore further the reason for the increase of the total damage. To do so, the following modeling steps were taken: (a) run the model assuming the combination of the high-flood scenario with the low-exposure scenario; (b) compare these results with the results of the high scenario (i.e., the combination of the high-flood scenario with the high-exposure scenario); (c) run the model assuming the combination of the low-flood scenario with the high-exposure scenario; and (d) compare these results with the results of the high scenario.

These comparisons show that the total economic damage increases between the high-flood-low-exposure scenario and the high scenario by a factor of 0.2, from a mean of 119.6 million USD to a mean of 141.8 million USD (Table 8). Direct and indirect damage to HPPs increases between the high-flood-low-exposure scenario and the high scenario by a factor of 4.7 (the highest factor across the four asset categories; from 3.9 million USD to 22 million USD).

Total economic damage increases between the low-flood-high-exposure scenario and the high scenario by a factor of 0.8, from a mean of 81 million USD to a mean of 141.8 million USD (Table 9). Direct and indirect damage to HPPs increases between the low-flood-high-exposure scenario and the high scenario by a factor of 0.1 (from 20.5 million USD to 22 million USD). Therefore, the increase of total economic damage between the low scenario and the high scenario is driven by the increase of two parameters: (a) the number of HPPs that could be damaged (i.e., from 7 to 18 HPPs) and (b) the extent of hazards.

A second important model result is that, considering direct damage only, HPPs and houses incur the highest mean economic damage for both scenarios. As shown in Tables 2 and 5, direct damage is split between the four asset categories for the low and high scenarios as follows: 16% and 53% for HPPs; 76% and 44% for houses; 8% and 3% for roads; and <1% for farmlands.

A third result is that, in a region where half of the population holds agricultural land smaller than 5,000 m^2, and subsistence agriculture is a common practice, direct

TABLE 1 Low scenario, mean economic value and standard deviation in brackets

Low scenario	HPP	Road	Settlement	Farmland	All assets
Direct damage	0.7 (0.8)	0.4 (<0.1)	3.6 (0.1)	<0.1 (<0.1)	4.7 (0.8)
Indirect damage	0.8 (0.8)	27.8 (3.2)	25.5 (2.9)	<0.1 (<0.1)	54.1 (6.2)
Total damage	1.5 (1.6)	28.2 (3.2)	29.1 (2.9)	<0.1 (<0.1)	58.8 (6.4)

Values are in million USD per damage type and asset category.

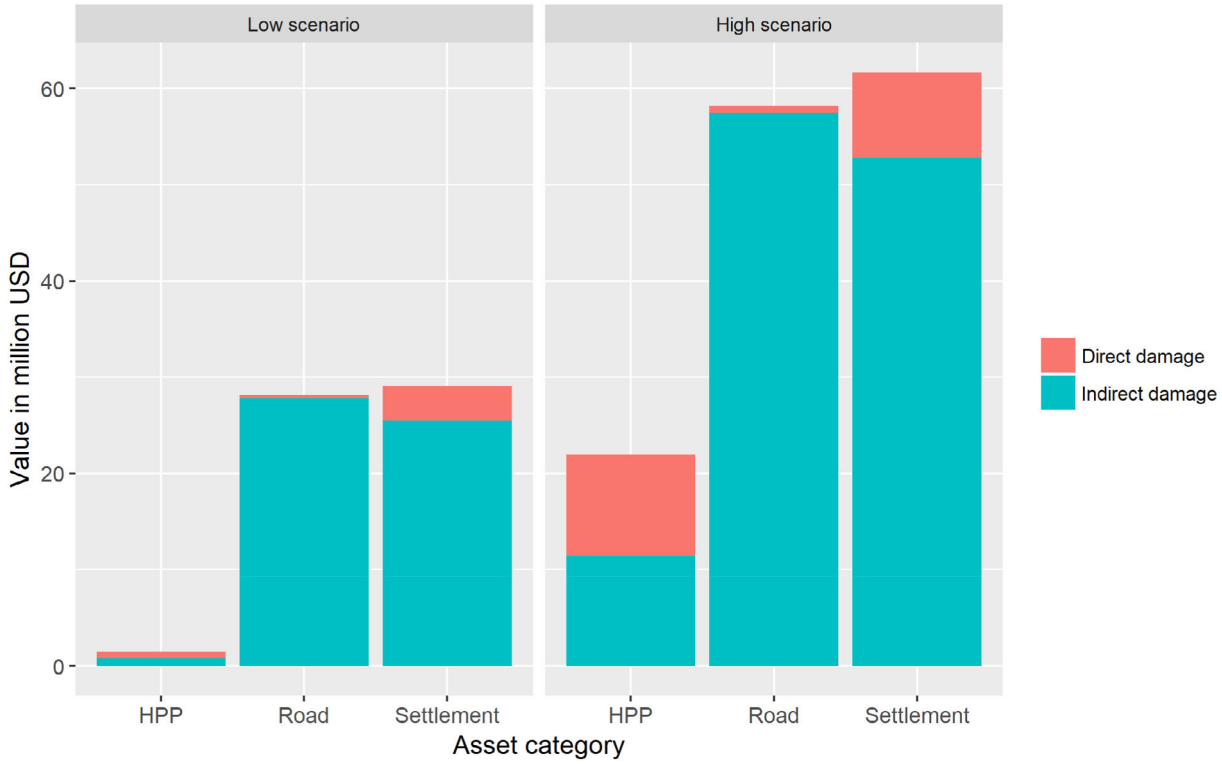

FIGURE 4 Stacked bar charts of the mean value of direct and indirect damage in million USD. The chart on the left shows damage for the low scenario. The chart on the right shows damage for the high scenario. In both charts, the *x*-axis represents the asset category. The asset category farmland is not displayed because of the small damage values that are modeled for this asset category

TABLE 2 Low scenario, contribution of asset category to damage type

Contribution of asset category to damage type (low scenario)	HPP	Road	Settlement	Farmland	All assets
Direct damage	16%	8%	76%	<1%	100%
Indirect damage	1%	51%	47%	<1%	100%
Total damage	3%	48%	49%	<1%	100%

and indirect damage to farmlands cannot be neglected, even though the estimated values for these damages are an order of magnitude lower than the estimated damage to the three other asset categories. The total damage to farmland is significantly lower because the modeled area of farmland vulnerable to floods and flood-induced landslides is small (1.2 km^2 for the low scenario and 1.9 km^2 for the high scenario) and the economic value per pixel is much lower for farmland than for the three other asset categories.

A fourth important model result is that, for both scenarios, flood risk is largely associated with the threat of road closures, which result in the loss of income for villagers and the loss of customs revenues. In the low and high scenarios, respectively, 92% and 86% of the damage summed over all four asset categories is indirect (Tables 3 and 6). In both scenarios, the categories road and settlement have the largest share of indirect damage (Tables 2 and 5). In the low scenario, the loss of customs revenue owing to road closures (27.8 million USD) contributes

TABLE 3 Low scenario, contribution of damage type to asset category

Contribution of damage type to asset category (low scenario)	HPP	Road	Settlement	Farmland	All assets
Direct damage	48%	1%	12%	33%	8%
Indirect damage	52%	99%	88%	67%	92%
Total damage	100%	100%	100%	100%	100%

High scenario	HPP	Road	Settlement	Farmland	All assets
Direct damage	10.6 (9.2)	0.7 (<0.1)	8.9 (0.2)	<0.1 (<0.1)	20.1 (9.2)
Indirect damage	11.4 (9.4)	57.5 (4.4)	52.8 (4.0)	<0.1 (<0.1)	121.7 (12.4)
Total damage	22.0 (18.3)	58.2 (4.4)	61.7 (4.0)	<0.1 (<0.1)	141.8 (19.8)

Values are in million USD per damage type and asset category.

TABLE 4 High scenario, mean economic value and standard deviation in brackets

TABLE 5 High scenario, contribution of asset category to damage type

Contribution of asset category to damage type (high scenario)	HPP	Road	Settlement	Farmland	All assets
Direct damage	53%	3%	44%	<1%	100%
Indirect damage	9%	47%	43%	<1%	100%
Total damage	16%	41%	43%	<1%	100%

TABLE 6 High scenario, contribution of damage type to asset category

Contribution of damage type to asset category (high scenario)	HPP	Road	Settlement	Farmland	All assets
Direct damage	48%	1%	14%	33%	14%
Indirect damage	52%	99%	86%	67%	86%
Total damage	100%	100%	100%	100%	100%

TABLE 7 Difference between results from low and high scenarios (in million USD and %)

Difference from low scenario to high scenario, mean value in million USD	HPP	Road	Settlement	Farmland	All assets
Direct damage	9.8	0.3	5.3	<0.1	15.4
Indirect damage	10.6	29.7	27.3	<0.1	67.7
Total damage	20.5	30	32.6	<0.1	83.1
Factor of increase relative to low scenario	14.5	2.1	2.1	1.5	2.4
Contribution of asset category to difference in total damage	25%	36%	39%	<1%	100%

51% to indirect damage (Tables 1 and 2). The loss of income from road traffic for the local population (25.5 million USD) contributes 47% to indirect damage. In the high scenario, the loss of customs revenue owing to road closures of 57.5 million USD contributes 47% to indirect damage (Tables 4 and 5). The loss of 52.8 million USD of income from road traffic for the local population contributes 43% to indirect damage. As such, damage owing to road closures contributes 98% and 90% to indirect damage, for the low and high scenarios respectively.

TABLE 8 Comparison between the results from the high-flood-low-exposure scenario (i.e., the combination of the high-flood scenario and the low-exposure scenario) and those from the high scenario

High-flood-low-exposure scenario and comparison, mean value in million USD	HPP	Road	Settlement	Farmland	All assets
Total damage, alternative scenario (A)	3.9	58.3	57.4	<0.1	119.6
Total damage, high scenario (B)	22.0	58.2	61.7	<0.1	141.8
Absolute stand-alone effect of high exposure (C = B − A)	18.1	<0.1	4.3	<0.1	22.2
Factored stand-alone effect of high exposure (C/A)	4.7	<0.1	0.1	<0.1	0.2

TABLE 9 Comparison between the results from the low-flood-high-exposure scenario (i.e., the combination of the low-flood scenario and the high-exposure scenario) and those from the high scenario

Low-flood-high-exposure scenario and comparison, mean value in million USD	HPP	Road	Settlement	Farmland	All assets
Total damage, alternative scenario (A)	20.5	28.0	32.5	<0.1	81.0
Total damage, high scenario (B)	22.0	58.2	61.7	<0.1	141.8
Absolute stand-alone effect of high flood (C = A − B)	1.4	30.2	29.2	<0.1	60.8
Factored stand-alone effect of high flood (C/A)	0.1	1.1	0.9	0.5	0.8

5 | DISCUSSION AND CONCLUSION

Important limitations of this work pertain to modeling uncertainties, owing in part to the lack of data for the study area and the highly parameterised modeling approaches used. For example, the estimation of the indirect damage to roads based only on direct damage to this asset category is arguably crude. In fact, the duration and severity of traffic disruption after destructive flood events are influenced not only by direct damages but also by the availability of alternative means of transportation (e.g., on foot and by donkey) and the distance between the damaged road sections.

Despite modeling uncertainties, the results show that flood risk in terms of economic damage is severe in the study area, and more so for the high scenario than for the low scenario. As this paper aims to provide methods for assessing flood risk in Nepal, we conclude by pointing to the following suggestions toward improving the methods proposed in this study, which could be implemented in future work: (a) working with loss exceedance curves; (b) adding human death to the types of consequences that are modeled; and (c) developing FRAMs for areas that share characteristics with the study area of this work.

In this work, flood risk is assessed in terms of economic damage for two combinations of flood and exposure scenarios that are not assigned a probability of occurrence although such an assignment is typical for flood risk assessments. As such, future studies that include the derivation of both damage functions and raster layers of water depth associated with probabilities of occurrence could focus on estimating flood risk in terms of the expected annual damage, which would be derived by integrating a loss exceedance curve (i.e., a function where the damage depends on an exceedance probability).

Besides, some consequences of floods and flood-induced landslides that might affect livelihoods, such as human fatalities and casualties, are not considered in this study, even though past consequences of floods in the Koshi Basin include the death of people and methods have been proposed to model flood risk in terms of loss of life (e.g., in Chen et al., 2013; Jonkman & Vrijling, 2002; Brázdová & Říha, 2014; Jonkman, Vrijling, & Vrouwenvelder, 2008). Therefore, future work related to flood risk in Nepal could focus on the model-based assessment of flood risk expressed in terms of fatalities, in addition to economic damage.

Finally, the study area of this work is only one of the many parts of Nepal that recurrently witness flood disasters. As such, we advocate that local assessments of flood risk in terms of economic damage are performed by drawing from the methods proposed in this paper, and that these local assessments are aggregated for the whole of Nepal. In addition, the aggregation of local assessments should be carried out for areas outside Nepal that have the same following characteristics of our case study: (a) high flood risk is left unaddressed; (b) the majority of the population would strongly benefit from more secure livelihoods; (c) there is a lack of financial resources that are allocated to measures for flood risk reduction; and (d) data related to flood risk (e.g., survey data after flood

disasters and hydrological data) are scarce. Examples of these countries in Asia include most countries in the Hindu Kush Himalayan region and many upland regions in South East Asian countries. It is hoped that the application of the methods of this work to other relevant study areas will increase the awareness of stakeholders, including governments, of the importance of, and therefore speed up action towards, improved measures for flood risk reduction.

ACKNOWLEDGEMENTS

This study was partially supported by funds of the National University of Singapore (NUS) and Yale-NUS. This study was also partially supported by core funds of ICIMOD contributed by the governments of Afghanistan, Australia, Austria, Bangladesh, Bhutan, China, India, Myanmar, Nepal, Norway, Pakistan, Switzerland, and the United Kingdom. The views and interpretations in this publication are those of the authors, and do not imply the expression of any opinion by ICIMOD, NUS, and Yale-NUS concerning the legal status of any country, territory, city or area of its authority, or concerning the delimitation of its frontiers or boundaries, or the endorsement of any product.

CONFLICT OF INTEREST

The authors have no competitive interests to declare.

DATA AVAILABILITY STATEMENT

The data that support the findings of this study are available on request from the corresponding author. The data are not publicly available due to privacy or ethical restrictions.

REFERENCES

ADPC. (2015). *Nepal hazard risk assessment part 1. Asian Disaster Preparedness Center, Norwegian Geotechnical Institute, and Centre for International Studies and Cooperation*. ADPC.

Agoshkov, V. I. (2002). *Mathematical models of support systems. Knowledge for sustainable development: An insight into the Encyclopedia of life support systems*. UNESCO/EOLSS.

Arnell, N. W. (1989). Expected annual damages and uncertainties in flood frequency estimation. *Journal of Water Resources Planning and Management*, *115*, 94–108.

Bhandari, N. B., Bhattarai, D., & Aryal, M. (2015). *Cost, production and price spread of cereal crops in Nepal: A time series analysis (2014/2015)*. Ministry of Agriculture Development, Department of Agriculture.

Bloomberg Markets. 2017. *USDNPR Spot Exchange Rate. 5Y. Rate on the April 17, 2015*. [online]. Retrieved from https://www.bloomberg.com/quote/USDNPR:CUR

Bookhagen, B., & Burbank, D. W. (2006). Topography, relief, and TRMM-derived rainfall variations along the Himalaya. *Geophysical Research Letters*, *33*, 1–5.

Brázdová, M., & Říha, J. (2014). A simple model for the estimation of the number of fatalities due to floods in Central Europe. *Natural Hazards and Earth System Sciences*, *14*, 1663–1676.

CBS. (2013). *Central Bureau of Statistics of Nepal: National Sample Census of agriculture, 2011/12*. Sindhupalchowk, Nepal: CBS.

CBS. (2014a). *Central Bureau of Statistics of Nepal, National Population and housing census 2011 (village development committee/municipality)*. Sindhupalchowk, Nepal: CBS.

CBS. (2014b). *Central Bureau of Statistics of Nepal: Population Monograph of Nepal – Volume I – Population dynamics*. Sindhupalchowk, Nepal: CBS.

CBS. (2014c). *Central Bureau of Statistics of Nepal: Population Monograph of Nepal – Volume III – Economic demography*. Sindhupalchowk, Nepal: CBS.

Chen, N., Hu, G., Deng, W., Khanal, N., Zhu, Y. H., & Han, D. (2013). On the water hazards in the trans-boundary Kosi River basin. *Natural Hazards and Earth System Sciences*, *13*, 795–809.

Cook, K., Andermann, C., Gimbert, F., Hovius, N. & Adhikari, B. 2017. *Geophysical research abstracts, impacts of the 2016 outburst flood on the Bhote Koshi River valley, Central Nepal*.

CRED. 2016. *Centre for Research on the Epidemiology of Disasters, Country Profile in EM-DAT and Disaster list* [Online]. Retrieved from http://www.emdat.be/country_profile/index.html; http://www.emdat.be/disaster_list/index.html

Dahal, R. K., & Bhandary, N. P. (2013). *Geo-disaster and its mitigation in Nepal. Progress of geo-disaster mitigation technology in Asia*, Berlin, Heidelberg: Springer.

Delalay, M. 2018. *Cloud FRAM* [Online]. Retrieved from https://github.com/mdelalay

Delalay, M., Tiwari, V., Ziegler, A. D., Gopal, V., & Passy, P. (2019). Land-use and land-cover classification using Sentinel-2 data and machine-learning algorithms: Operational method and its implementation for a mountainous area of Nepal. *Journal of Applied Remote Sensing*, *13*, 1–16.

Delalay, M., Ziegler, A. D., Shrestha, M. S., Wasson, R. J., Sudmeier-Rieux, K., Mcadoo, B. G., & Kochhar, I. (2018). Towards improved flood disaster governance in Nepal: A case study in Sindhupalchok District. *International Journal of Disaster Risk Reduction*, *31*, 354–366.

Devkota, K. C., Regmi, A. D., Pourghasemi, H. R., Yoshida, K., Pradhan, B., Ryu, I. C., … Althuwaynee, O. F. (2013). Landslide susceptibility mapping using certainty factor, index of entropy and logistic regression models in GIS and their comparison at Mugling–Narayanghat road section in Nepal Himalaya. *Natural Hazards*, *56*, 299–320.

Dhakal, S. (2015). *Chapter 4: Evolution of geomorphologic hazards in Hindu Kush Himalaya Mountain hazards and disaster risk reduction*. Tokyo, Japan: Springer.

Digital Globe. 2017. *Google Earth Pro* [online]. Retrieved from https://www.digitalglobe.com/

Dixit, A. (2009). Kosi embankment breach in Nepal: Need for a paradigm shift in responding to floods. *Economic and Political Weekly*, *44*, 70–78.

DoED. 2017. *Department of Electricity Development, Government of Nepal, Ministry of Energy, Issued Licenses and List of Applications* [Online]. Retrieved from http://www.doed.gov.np/

Drab, A., & Riha, J. (2010). An approach to the implementation of European directive 2007/60/EC on flood risk management in The Czech Republic. *Natural Hazards and Earth System Sciences*, *10*, 1977–1988.

Feyen, L., Dankers, R., & Bódis, K. (2011). Fluvial flood risk in Europe in present and future climates. *Journal of Climatic Change*, *112*, 47–62.

Gaire, S., Castro Delgado, R., & Arcos González, P. (2015). Disaster risk profile and existing legal framework of Nepal: Floods and landslides. *Risk Management and Healthcare Policy*, *8*, 139–150.

Gautam, D., Prajapati, J., Paterno, K. V., Bhetwal, K. K., & Neupane, P. (2016). Disaster resilient vernacular housing technology in Nepal. *Geoenvironmental Disasters*, *3*, 1–14.

Gerl, T., Kreibich, H., Franco, G., Marechal, D., & Schröter, K. (2016). A review of flood loss models as basis for harmonization and benchmarking. *PLoS One*, *11*, 1–22.

Grossi, P., Kunreuther, H. & Patel, C. C. 2005. *Catastrophe modeling: A new approach to managing risk*. New York, NY: Springer Science+Business Media.

ICIMOD. 2017a. *International Centre for Integrated Mountain Development, Geological data of Nepal's Gorkha Earthquake 2015 affected area, RDS* [Online]. Retrieved from http://rds.icimod.org/Home/DataDetail?metadataId=24676

ICIMOD. 2017b. *International Centre for Integrated Mountain Development, Landslide data of 14 earthquake affected prioritized districts, RDS* [Online]. Retrieved from http://rds.icimod.org/Home/DataDetail?metadataId=31016

ICIMOD. 2017c. *International Centre for Integrated Mountain Development, Regional Database System* [Online]. Retrieved from http://rds.icimod.org/

IDS-Nepal, PAC, & GCAP. (2014). *Economic impact assessment of climate change in key sectors in Nepal*. IDS-Nepal.

Jaquet, S., Schwilch, G., Hartung-Hofmann, F., Adhikari, A., Sudmeier-Rieux, K., Shrestha, G., ... Kohler, T. (2015). Does outmigration lead to land degradation? Labour shortage and land management in a western Nepal watershed. *Applied Geography*, *62*, 157–170.

Jonkman, S. N., & Vrijling, J. K. (2002). Loss of life due to floods. *Journal of Flood Risk Management*, *1*, 43–56.

Jonkman, S. N., Vrijling, J. K., & Vrouwenvelder, A. C. W. M. (2008). Methods for the estimation of loss of life due to floods: A literature review and a proposal for a new method. *Natural Hazards*, *46*, 353–389.

Kansakar, S. R., Hannah, D. M., Gerrard, J., & Rees, G. (2004). Spatial pattern in the precipitation regime of Nepal. *International Journal of Climatology*, *24*, 1645–1660.

Kargel, J. S., Leonard, G. J., & Shugar, D. H. (2016). Geomorphic and geologic controls of geohazard induced by Nepal's 2015 Gorkha earthquake. *Science*, *351*, 140–152.

Kayastha, P., Dhital, M. R., & DE Smedt, F. (2013). Evaluation of the consistency of landslide susceptibility mapping: A case study from the Kankai watershed in East Nepal. *Landslides*, *10*, 785–800.

Kelman, I. (2015). Climate change and the Sendai framework for disaster risk reduction. *International Journal of Disaster Risk Science*, *6*, 117–127.

Khanal, N. R., Hu, J.-M., & Mool, P. (2015). Glacial Lake outburst flood risk in the Poiqu/Bhote Koshi/sun Koshi River basin in the Central Himalayas. *Mountain Research and Development*, *35*, 351–366.

Koks, E. E., Bočkarjova, M., Moel, H. D., & Aerts, J. C. J. H. (2014). Integrated direct and indirect flood risk modeling: Development and sensitivity analysis. *Risk Analysis*, *35*, 882–900.

Ligtvoet, W., Jongman, B., Bierkens, M. F. P., Winsemius, H. C., Bouwman, A., Sperna Weiland, F., ... Ward, P. J. (2013). Assessing flood risk at the global scale: Model setup, results, and sensitivity. *Environmental Research Letters*, *8*, 1–11.

Lutz, A. F., Immerzeel, W. W., Shrestha, A. B., & Bierkens, M. F. P. (2014). Consistent increase in high Asia's runoff due to increasing glacier melt and precipitation. *Nature Climate Change*, *4*, 587–594.

Malego, N. G., & Upreti, B. N. (2015). *Nepal Disaster Report 2015*. Nepal: The Government of Nepal, Ministry of Home Affairs (MoHA) and Disaster Preparedness Network-Nepal (DPNet-Nepal).

McGrath, H., Bourgon, J.-F., Proulx-Bourque, J.-S., Nastev, M., & Abo El Ezz, A. (2018). A comparison of simplified conceptual models for rapid web-based flood inundation mapping. *Natural Hazards*, *93*, 905–920.

de Moel, H., Jongman, B., Kreibich, H., Merz, B., Penning-Rowsell, E. & Ward, P. J. 2015. Flood risk assessments at different spatial scales. *Mitigation and Adaptation Strategies for Global Change,* Volume *20*, 865–890.

de Moel, H., VAN Alphen, J. & Aerts, J. C. J. H. 2009. Flood maps in Europe – Methods, availability and use. *Natural Hazards and Earth System Sciences 9*, 289–301.

Muis, S., Guneralp, B., Jongman, B., Aerts, J. C. J. H., & Ward, P. J. (2015). Flood risk and adaptation strategies under climate change and urban expansion: A probabilistic analysis using global data. *Science of the Total Environment*, *538*, 445–457.

Neupane, K., Dhakal, U., Acharya, S. H., Pandey, C. P., Singh, V. P. & Shrestha, D. H. D. 2018. *Nepal Disaster Report 2017*.

OECD. (2016). *Insuring flood risk. Organisation for Economic Co-operation and Development, Financial Management of Flood Risk*, Paris: OECD Publishing.

R Foundation. 2017. *What is R?* [Online]. Retrieved from https://www.r-project.org/about.html

Rasul, G. (2015). Water for growth and development in the Ganges, Brahmaputra, and Meghna basins: An economic perspective. *International Journal of River Basin Management*, *13*, 1814–2060.

Regmi, A. D., Cui, P., Dhital, M. R., & Zou, Q. (2016). Rock fall hazard and risk assessment along Araniko highway, Central Nepal Himalaya. *Environmental Earth Sciences*, *75*, 1112–1132.

Rimal, B., Baral, H., Stork, N. E., Paudyal, K., & Rijal, S. (2015). Growing City and rapid land use transition: Assessing multiple hazards and risks in the Pokhara Valley, Nepal. *Land*, *4*, 957–978.

Rounce, D. R., Mckinney, D. C., Lala, J. M., Byers, A. C., & Watson, C. S. (2016). A new remote hazard and risk assessment framework for glacial lakes in the Nepal Himalaya. *Hydrology and Earth System Sciences*, *20*, 3455–3475.

Schwanghart, W., Worni, R., Huggel, C., Stoffel, M., & Korup, O. (2016). Uncertainty in the Himalayan energy–water nexus: Estimating regional exposure to glacial lake outburst floods. *Environmental Research Letters*, *11*, 1–10.

Shaw, R., & Rahman, A.-U. (2015). Chapter 3: Floods in the hindu kush region: Causes and socio-economic aspects. In *Mountain hazards and disaster risk reduction*. Tokyo, Japan: Springer.

Shrestha, B. B., & Nakagawa, H. (2016). Hazard assessment of the formation and failure of the Sunkoshi landslide dam in Nepal. *Natural Hazards*, *82*, 2029–2049.

Smith, D. I. (1981). Actual and potential flood damage: A case study for urban Lismore, NSW, Australia. *Applied Geography*, *1*, 31–39.

Smith, D. I. (1994). Flood damage estimation – A review of urban stage-damage curves and loss functions. *Water SA*, *20*, 231–239.

Swiss Re. (2003). *Natural catastrophes and reinsurance*. Swiss Re.

Swiss Re. (2012). *Flood in Switzerland – An underestimated risk*. Swiss Re.

UNDP. (2014). *United Nations development Programme, Nepal, human development report 2014*. UNDP.

United Nations. (2015). *Sendai framework for disaster risk reduction 2015–2030*. United Nations.

USGS. 2017. *Earth explorer* [Online]. Retrieved from https://earthexplorer.usgs.gov/

Wilson, M., Bates, P., Alsdorf, D., Forsberg, B., Horritt, M., Melack, J., ... Famiglietti, J. (2007). Modeling large-scale inundation of Amazonian seasonally flooded wetlands: A 2D hydrodynamic model of the Amazon. *Geophysical Research Letters*, *34*, 1–6.

Woo, G. (2011). *Calculating catastrophe*, London, England: Imperial College Press.

How to cite this article: Delalay M, Ziegler AD, Shrestha MS, Gopal V. Methodology for future flood assessment in terms of economic damage: Development and application for a case study in Nepal. *J Flood Risk Management*. 2020;e12623. https://doi.org/10.1111/jfr3.12623